Q estimation from reflection seismic data for hydrocarbon detection using a modified frequency shift method

2015 J. Geophys. Eng. 12 577

(http://iopscience.iop.org/1742-2140/12/4/577)

IOP Publishing Journal of Geophysics and Engineering
J. Geophys. Eng. **12** (2015) 577–586 doi:10.1088/1742-2132/12/4/577

Q estimation from reflection seismic data for hydrocarbon detection using a modified frequency shift method

Fangyu Li[1], Huailai Zhou[2], Nan Jiang[3], Jianxia Bi[4] and Kurt J Marfurt[5]

[1] Conoco Phillips School of Geology and Geophysics, The University of Oklahoma, Norman, OK 73019, USA
[2] State Key Laboratory of Oil and Gas Reservoir Geology and Exploitation, Key Lab of Earth Exploration and Information Techniques of Ministry of Education, College of Geophysics, Chengdu University of Technology, Chengdu, Sichuan 610059, People's Republic of China
[3] School of Geoscience and Technology, Southwest Petroleum University, Chengdu, Sichuan 610500, People's Republic of China
[4] Exploration and Development Research Institute of Zhongyuan Oilfield Company of SINOPEC, Puyang, Henan 457001, People's Republic of China
[5] ConocoPhillips School of Geology and Geophysics, The University of Oklahoma, Norman, OK 73019, USA

E-mail: kmarfurt@ou.edu, fangyu.li@ou.edu, bjx_@163.com, zhouhuailai06@cdut.cn and dou_508@126.com

Received 23 December 2014, revised 23 April 2015
Accepted for publication 11 May 2015
Published 4 June 2015

Abstract

As a powerfully diagnostic tool for structural interpretation, reservoir characterization, and hydrocarbon detection, quality factor Q provides useful information in seismic processing and interpretation. Popular methods, like the spectral ratio (SR) method, central frequency shift (CFS) method and peak frequency shift (PFS) method, have their respective limitations in dealing with field seismic data. The lack of a reliable method for estimating Q from reflection seismic data is an issue when utilizing the Q value for hydrocarbon detection. In this article, we derive an approximate equation and propose a dominant and central frequency shift (DCFS) method by combining the quality factor Q, the travel time, and dominant and central frequencies of two successive seismic signals along the wave propagating direction. Based on multi-layered analysis, we then proposed a method to obtain continuous volumetric Q estimation results. A test using synthetic data and statistical experiments showed the proposed method can achieve higher accuracy and robustness compared with existing methods. Application of field data also shows its potential and effectiveness to estimate seismic attenuation.

Keywords: seismic attenuation, quality factor, Q estimation, hydrocarbon detection

(Some figures may appear in colour only in the online journal)

Introduction

Seismic attenuation is a fundamental mechanism of elastic waves propagating through the Earth. Attenuation acts as a time-variant low-pass filter with a monotonically increasing phase spectrum, which leads to the seismic wavelet becomes more stretched and its amplitude becoming exponentially smaller with time or depth. The quality (Q) factor is usually the measure of seismic attenuation.

Attenuation, if quantified, can be used as a seismic attribute to characterize rock properties, reservoir heterogeneity, subtle geological structures, and the success of completion processes (Parra and Hackert 2002, Korneev *et al* 2004). For example, in fractured media, the magnitude of attenuation change with

azimuth has been shown to be a useful indicator of fracture direction (Clark *et al* 2001, Maultzsch *et al* 2007); attenuation is sensitive to changes in gas saturation in partially saturated media (Winkler and Nur 1982), so anomalously high attenuation can be viewed as a hydrocarbon indicator (Toksöz *et al* 1979, Hedlin *et al* 2001), especially if quantitative attenuation measurements can be made. Once attenuation is measured, it is possible to mitigate the resolution loss by applying processes such as inverse-Q filtering to raise the high-frequency content of later times in seismic sections to compensate for attenuation of the seismic wave (Wang 2002, Zhang and Ulrych 2002, Wang 2006, Wang 2008) to aid with structural interpretations (Kaderali *et al* 2007), amplitude versus offset (AVO) analysis (Luh 1993), and anisotropic attenuation characterization (Maultzsch *et al* 2007, Zhu and Tsvankin 2007). Therefore, attenuation can provide important information about the subsurface to facilitate seismic interpretation.

The anelasticity and inhomogeneity in the subsurface dissipate high-frequency seismic energy, causing a decrease in seismic amplitude as a consequence. Based on these observations, much research has been performed for Q estimation. The first proposed technique was the wavelet broadening technique by Ricker (1953). In the time domain, the Q factor is usually estimated by pulse amplitude decay (Brzostowski and McMechan 1992), pulse rising time (Kjartansson 1979), and pulse broadening (Wright and Hoy 1981), which all use pulse amplitude information. Nevertheless, amplitude information of seismic pulses is often influenced by scattering, geometric spreading, and other factors. In the frequency domain, approaches of the Q estimation include the spectral ratio (SR) (Hauge 1981, Raikes and White 1984, Sams and Goldberg 1990, White 1992), central frequency shift (CFS) (Quan and Harris 1997), peak frequency shift (PFS) (Zhang and Ulrych 2002), improved peak frequency shift (IPFS) (Hu *et al* 2013), and Gabor-Morlet joint time frequency analysis (JTFA) (Singleton *et al* 2006) methods, all of which require time-frequency transforms to calculate the spectra of seismic records. Additionally, Q can also be estimated by variation of instantaneous frequency (IF) of a seismic signal. Barnes (1991), Tonn (1991), and Engelhard (1996) obtained the relationship between the measured instantaneous spectra and seismic attenuation. Matheney and Nowack (1995) proposed the IF matching (IFM) method. Li *et al* (2006) suggested using peak scale variations in the wavelet domain to estimate Q by assuming an idealized pulse as the seismic source wavelet. In addition, especially for reflection seismic data Q estimation, there is another group of 'stable' methods (Wang 2004, Wang 2014) based on the integral rather than differential (ratio) and presented as a 1D function of the product of frequency and time.

Among the many methods available for measuring seismic attenuation, frequency-based methods are common in exploration of geophysics because of their reliability and ease of use. The most classic approach is the spectral ratio (SR) method, which measures the log of the ratio between two amplitude spectra computed as function of frequency. However, the SR method would be easily affected by noise. The frequency-shift methods, such as central frequency shift and peak frequency shift methods, only use the variations of the spectra rather than the entire amplitude spectrum, thus improving the accuracy of the estimation.

In this article, we first analyze the presuppositions of the CFS and PFS methods. Then, we derive an approximate equation combining Q and variance of dominant and central frequencies, and propose a method called the dominant and central frequency shift (DCFS) method. The hypothesis of the proposed method is more practical and satisfies the basic characteristics of the seismic signal, which provides the basis of reasonable accuracy and robustness. Finally, we calibrate the proposed method for both synthetic and field seismic data.

Existing methods and their preconditions

The underlying theory of Q and associated measurement methods are well-established (White 1992, Reine *et al* 2009). For frequency-independent intrinsic Q in the bandwidth of interest, a seismic signal will have its spectral amplitude $A_0(f)$ modified to $A_1(f)$ after travelling time t at frequency f:

$$A_1(f) = A_0(f)\exp(-\pi ft/Q), \tag{1}$$

where the amplitude decay or increase caused by frequency-independent effects, which can be cancelled or balanced in frequency domain, is ignored. The observed difference in the frequency spectrum of a Ricker seismic pulse at 0 s and time t = 0.1 s are shown in figure 1, when the source wavelet propagates through the attenuating medium with a different Q value.

Based on equation (1), the SR method can be represented as

$$\ln\left(\frac{|A_1(f)|}{|A_0(f)|}\right) = -\pi ft/Q. \tag{2}$$

An estimate of Q can be derived by curve fitting within the common effective bandwidth of the two spectra using the least-squares method. An effective bandwidth should be chosen to avoid high-frequency fluctuation caused by additive noise or numerical errors introduced by finite precision.

Quan and Harris (1997) proposed the CFS method by correlating Q with the changes in the central frequency of the seismic signal. For the reference seismic signal A_0 and the target seismic signal A_1, their central frequencies are denoted by f_{c_0} and f_{c_1}; assuming that $|A(f)|$ is of Gaussian shape, and Q can be quantified by

$$Q = \frac{\pi t\sigma_{A_0}^2}{f_{c_0} - f_{c_1}}, \tag{3}$$

where $\sigma_{A_0}^2$ is the spectrum variance of A_0, defined by

$$\sigma_{A_0}^2 = \frac{\int_0^\infty (f - f_{c_0})^2 |A_0(f)|\mathrm{d}f}{\int_0^\infty |A_0(f)|\mathrm{d}f}. \tag{4}$$

As an alternate Q estimation method of SR methods, the CFS method is a milestone for frequency shift methods. It is quite robust because the estimation of central frequency is not as sensitive to noise as the SR method. However, we

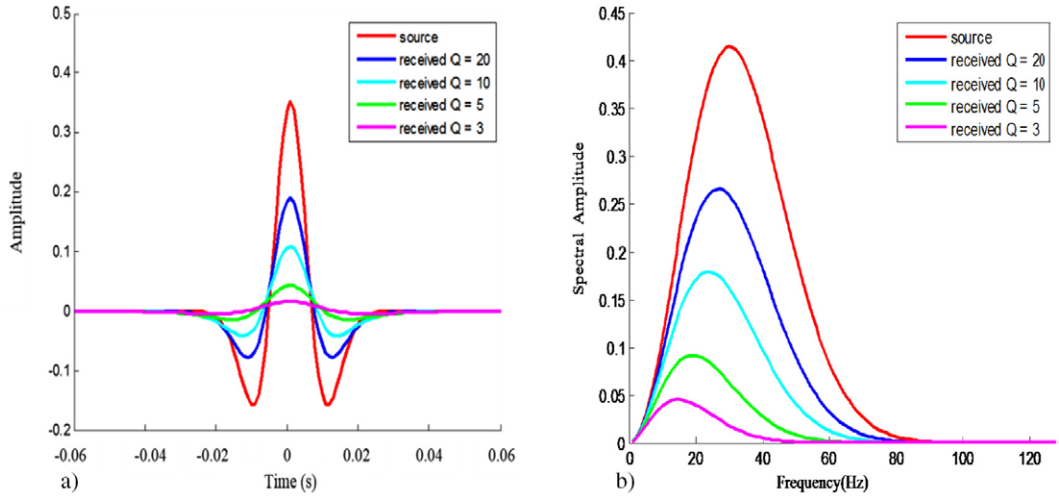

Figure 1. The time domain expressions (a) and frequency spectra (b) of a Ricker wavelet with 30 Hz dominant frequency at time 0 (red) and time $t = 0.1$ s in different attenuating mediums with different Q values; the loss in frequency and amplitude reduction due to the effect of attenuation are shown.

notice that the preconditions of the CFS method are the Gaussian shape of the seismic spectrum and the unchanged spectrum variance. (Admittedly, rectangular and triangular spectral shape situations were also considered using the CFS method, but they are even further away from being realistic.) However, the seismic spectrum is usually a non-Gaussian distribution and the attenuation effect would certainly change the spectrum variance, which brings inaccuracies to this method.

Zhang and Ulrych (2002) proposed another frequency shift method, namely the PFS method, by correlating Q with the changes in the peak frequency of the seismic wavelets. The peak frequency literally means the frequency corresponding to the maximal value of the spectra amplitude.

For the reference wavelet b_0 and the target wavelet b_1, their peak frequencies are denoted by f_{p_0} and f_{p_1}; assuming that the seismic source can be represented by a Ricker wavelet, an estimate of Q can be quantified by

$$Q = \frac{\pi t f_{p_1} f_{p_0}^2}{2(f_{p_0}^2 - f_{p_1}^2)}. \tag{5}$$

The spectrum of a Ricker wavelet (Ricker, 1953) is

$$A(f) = \frac{2}{\sqrt{\pi}} \frac{f^2}{f_m^3} \exp\left(-\frac{f^2}{f_m^2}\right), \tag{6}$$

where f_m is the dominant frequency of the wavelet.

The peak frequency is the dominant frequency for a Ricker wavelet. The PFS method is reasonable because we are simply not able to set up any kind of relationship between Q and frequency shift without certain *a priori* information. Compared with the Gaussian shape assumption, the Ricker wavelet assumption is made much more often and is thus more widely accepted. However, the identification of the maximal value of the spectra amplitude is easily affected by the background noise, which cannot be ignored. Thus, the PFS method always seems unstable in the field application, whereas CFS is more robust because the central frequency estimation is quite insensitive to noise.

Dominant and central frequency shift method

To better face actual field situations, by combining the advantages of CFS and PFS we evaluated the amplitude spectrum variance by central frequency shift through time modeled as a Ricker wavelet traveling, as in equation (6). Combining equations (1) and (6), by considering the seismic wave propagating in the Earth media with a Q factor for t seconds, we can obtain the amplitude spectrum of the received signal as

$$A(f,t) = \frac{2}{\sqrt{\pi}} \frac{f^2}{f_m^3} e^{-\frac{f^2}{f_m^2}} e^{-\frac{\pi f t}{Q}}, \tag{7}$$

where f_m denotes the dominant frequency of the source wavelet.

The central frequency of a signal $s(t)$ is usually defined as

$$f_c = \frac{\int_0^\infty f \cdot \mathrm{S}(f)\mathrm{d}f}{\int_0^\infty \mathrm{S}(f)\mathrm{d}f}, \tag{8}$$

where $\mathrm{S}(f)$ is the amplitude spectrum of signal $s(t)$.

However, Wang (2015) concluded that central frequency should be evaluated from the power spectrum rather than the amplitude spectrum, because the analytically derived expression has higher correspondence than the estimation retrieved from visual inspection of the discrete Fourier spectrum of the seismic data.

Likewise, the central frequency based on power spectrum is expressed as

$$f_c = \frac{\int_0^\infty f \cdot \mathrm{S}^2(f)\mathrm{d}f}{\int_0^\infty \mathrm{S}^2(f)\mathrm{d}f}. \tag{9}$$

Thus, the central frequency of the received seismic signal amplitude spectrum $A(f,t)$ is

$$f_c = \frac{\int_0^\infty f|A(f,t)|^2\,\mathrm{d}f}{\int_0^\infty |A(f,t)|^2\,\mathrm{d}f} = \frac{\int_0^\infty f\left(\frac{2}{\sqrt{\pi}}\frac{f^2}{f_m^3}\mathrm{e}^{-\frac{f^2}{f_m^2}}\mathrm{e}^{-\frac{\pi f t}{Q}}\right)^2\mathrm{d}f}{\int_0^\infty\left(\frac{2}{\sqrt{\pi}}\frac{f^2}{f_m^3}\mathrm{e}^{-\frac{f^2}{f_m^2}}\mathrm{e}^{-\frac{\pi f t}{Q}}\right)^2\mathrm{d}f}. \quad (10)$$

After simplifying equation (10), we can obtain

$$f_c = f_m\frac{\int_\alpha^\infty\left(x-\frac{\pi f_m t}{2Q}\right)^5\exp(-2x^2)\mathrm{d}x}{\int_\alpha^\infty\left(x-\frac{\pi f_m t}{2Q}\right)^4\exp(-2x^2)\mathrm{d}x}, \quad (11)$$

where $\alpha=\frac{\pi f_m t}{2Q}$, $x=\frac{f}{f_m}+\frac{\pi f_m t}{2Q}$.

Approximately, we obtain a relationship as follows

$$f_c = \frac{f_m}{2\sqrt{\pi}}\frac{\begin{array}{c}(\sqrt{\pi}-1)\left(\frac{\pi f_m t}{Q}\right)^6-\sqrt{2\pi}\left(\frac{\pi f_m t}{Q}\right)^5\\+(10\sqrt{\pi}-7)\left(\frac{\pi f_m t}{Q}\right)^4\\-10\sqrt{2\pi}\left(\frac{\pi f_m t}{Q}\right)^3+5(3\sqrt{\pi}+2)\left(\frac{\pi f_m t}{Q}\right)^2\\-15\sqrt{2\pi}\left(\frac{\pi f_m t}{Q}\right)+16\end{array}}{\begin{array}{c}\frac{\sqrt{\pi}-1}{\sqrt{\pi}}\left(\frac{\pi f_m t}{Q}\right)^5-\sqrt{2}\left(\frac{\pi f_m t}{Q}\right)^4+3\frac{1-2\sqrt{\pi}}{\sqrt{\pi}}\left(\frac{\pi f_m t}{Q}\right)^3\\+6\sqrt{2}\left(\frac{\pi f_m t}{Q}\right)^2-\frac{10\sqrt{\pi}+3\pi}{\pi}\left(\frac{\pi f_m t}{Q}\right)+3\sqrt{2}\end{array}}. \quad (12)$$

To verify the correctness of (12), we can compute the f_c of the source signal

$$f_c = \frac{\int_0^\infty f|A(f)|^2\,\mathrm{d}f}{\int_0^\infty |A(f)|^2\,\mathrm{d}f} = \frac{\int_0^\infty f\left(\frac{2}{\sqrt{\pi}}\frac{f^2}{f_m^3}\mathrm{e}^{-\frac{f^2}{f_m^2}}\right)^2\mathrm{d}f}{\int_0^\infty\left(\frac{2}{\sqrt{\pi}}\frac{f^2}{f_m^3}\mathrm{e}^{-\frac{f^2}{f_m^2}}\right)^2\mathrm{d}f} = \frac{\frac{1}{2\pi}}{\frac{3}{8\sqrt{2\pi}f_m}}$$
$$= \frac{4}{3}\sqrt{\frac{2}{\pi}}f_m. \quad (13)$$

When there is no attenuation, we can assume that time t equals 0 or Q equals infinity in equation (12); then, expression of central frequency of the source signal becomes

$$f_c = \frac{f_m}{2\sqrt{\pi}}\frac{16}{3\sqrt{2}} = \frac{4}{3}\sqrt{\frac{2}{\pi}}f_m, \quad (14)$$

which has the same form as equation (13). Therefore, our calculation and derivation for central frequency, dominant frequency, and Q in equation (12) are correct.

Because our goal is to estimate Q factor, we changed equation (12) to an equation about unknown parameter Q and solved it. Because that equation is a sixth-degree equation in one variable, we can only obtain the approximate solution,

$$Q \approx \frac{f_m^2\pi t}{4f_m\sqrt{\frac{2}{\pi}}-3f_c\sqrt{\pi}}. \quad (15)$$

The relationship between the central frequency, dominant frequency, and Q factor has been established. Thus, we can obtain the quality factor estimation, and this method is called the DCFS method. It is a modified CFS method; we substitute Gaussian spectrum with non-Gaussian spectrum of the Ricker wavelet, which is more coincident with the actual situation as wave propagates under the survey. In addition, because there is no variance parameter in the Ricker wavelet expression, we do not need to estimate the variance of the reference spectrum, thus allowing calculations to be more straightforward and suppressing the inaccuracy from ignorance of the shape difference between the reference and the received spectra.

Two aspects should be noticed: first, the constant Q model assumes that the attenuation effect is 'constant' in the target horizon, so we can only get an 'average' attenuation estimation; second, regardless of whether the CFS method or DCFS method is used, to fulfill the first-order Taylor approximation used during the simplification process, the travel time t should not be too large. Thus, when a target horizon is relatively thick, from both physical and mathematical aspects, we need to view it as a multi-layered model, separate it into some thin layers, and perform the Q estimation layer-by-layer (Zhang and Ulrych 2002, Wang 2008). When the time interval becomes smaller and smaller, the Q estimation result changes from constant, to discrete, to continuous. In the following section, we discuss how to implement the Q analysis algorithm in a multi-layered case, after which the attenuation estimation would become a volumetric instead of a strata attribute.

Multi-layered implementation

First, consider a case of two layers with quality factors Q_1 and Q_2 and travel times t_1 and t_2 in each layer, respectively, with the total travel time $t = t_1 + t_2$ and the total equivalent quality factor Q. Applying equation (1), we obtain

$$A(f,t) = A_0(f)\exp\left(\frac{-\pi f t}{Q}\right) = A_0(f)\exp\left(\frac{-\pi f t_1}{Q_1}\right)\exp\left(\frac{-\pi f t_2}{Q_2}\right). \quad (16)$$

Once knowing Q and Q_1, Q_2 can be expressed by

$$Q_2 = \frac{t_2 Q_1 Q}{(t_1+t_2)Q_1 - t_1 Q}. \quad (17)$$

From equation (16), the equivalent Q can be estimated using the dominant frequency of the source wavelet and central frequency at time t. Because the dominant frequency f_m of the initial wavelet and Q_1 have already been determined from upper-layer arrivals, and because the travel time parameters t_1 and t_2 can be estimated, Q_2 can be computed from equation (17).

Suppose that the subsurface medium is divided into N layers, separated at times $t_0, t_1, \cdots, t_i, \cdots, t_{N-1}, t$ with a total equivalent quality factor Q, then the amplitude spectrum is defined by

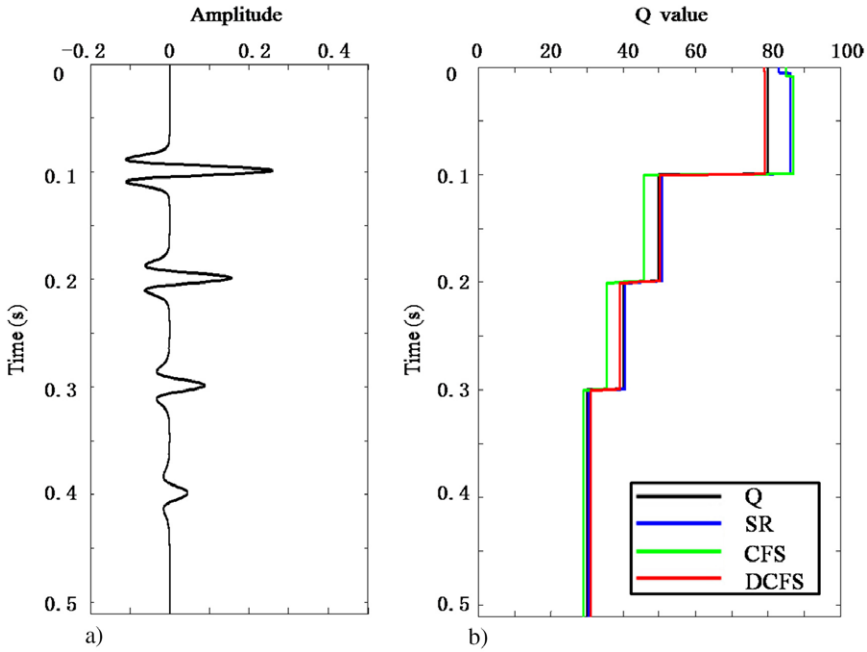

Figure 2. An example of Q estimation. (a) A noise-free synthetic seismogram generated by a 40 Hz Ricker wavelet in a layered medium in which each layer has a Q value of 80, 50, 40, and 30, respectively. (b) The results of Q estimation using SR, CFS, and DCFS methods.

$$A(f,t) = A_0(f)\exp\left(\sum_{i=1}^{N}\frac{-\pi f\Delta t_i}{Q_i}\right), \tag{18}$$

where $\Delta t_i = t_i - t_{i-1} \geq 0$ and Q_i are the travel time and quality factor in the ith layer, respectively.

For the last layer, which has thickness $\Delta t_N = t - t_{N-1}$, the amplitude spectrum is

$$A(f,t) = A_0(f)\exp\left(\sum_{i=1}^{N-1}\frac{-\pi f\Delta t_i}{Q_i}\right)\exp\left[\frac{-\pi f(t-t_{N-1})}{Q_N}\right]. \tag{19}$$

Similar to equation (17), we can obtain the equation for Q_N :

$$Q_N = \frac{\Delta t_N}{\frac{t}{Q} - \sum_{i=1}^{N-1}\frac{\Delta t_i}{Q_i}}. \tag{20}$$

Now, the Q factor values can be computed layer-by-layer. Then, we can obtain a 'continuous' attenuation estimation result.

To stabilize this procedure and make the result more robust and smooth, we can normalize the amplitude spectrum $A(f,t)$ between t_{n-1} and t_n, as

$$\hat{A}(f,t) = \begin{cases} \hat{A}(f,t_{n-1}), & \text{for } \exp\left(\sum_{i=1}^{n-1}\frac{-\pi f\Delta t_i}{Q_i}\right) \geq 1 \\ \dfrac{A(f,t)}{\exp\left(\sum_{i=1}^{n-1}\frac{-\pi f\Delta t_i}{Q_i}\right)}, & \text{for } \beta \leq \exp\left(\sum_{i=1}^{n-1}\frac{-\pi f\Delta t_i}{Q_i}\right) < 1 \\ 0, & \text{for } \exp\left(\sum_{i=1}^{n-1}\frac{-\pi f\Delta t_i}{Q_i}\right) < \beta \end{cases}, \tag{21}$$

where the threshold β is related to signal-to-noise ratio.

In this way, the small amplitude samples are ignored in the Q analysis, so we can suppress noise interference, which is more important, and the unphysical negative Q value can also be eliminated.

Synthetic test

To confirm the effectiveness and stability of our proposed method (DCFS), we estimated Q values in both noise-free and noise-added synthetic data and analyzed the results calculated by SR, CFS, and DCFS methods.

We used a Ricker wavelet with dominant frequency of 40 Hz to produce a noise-free synthetic seismogram in a layered medium, in which each layer has a Q value of 80, 50, 40, and 30, respectively, as shown in figure 2(a). The results of Q estimation obtained by SR, CFS, and DCFS methods show that three methods perform well in the noise-free case, as shown in figure 2(b). Note that the results using the DCFS method are obtained by combining equations (15), (20), and (21).

The most difficult problem is stability in evaluating the Q factor when the data are contaminated by noise. Therefore, we implemented the three aforementioned methods to calculate the Q values for the synthetic data (same as figure 2(a)) including different noise levels with SNR = 30, 10, 5, 0, and −1 dB, as shown in figure 3. We can observe from the results that there are noticeable differences between these three methods in a situation with high SNR. For the SR method, accuracy and stability of estimation highly depends on the SNR of original data. When SNR is less than 5 dB, the DCFS method performs more robustly, and the results calculated by DCFS are closer to the true Q values than those of the other two methods, as shown in figures 3(h) and (j).

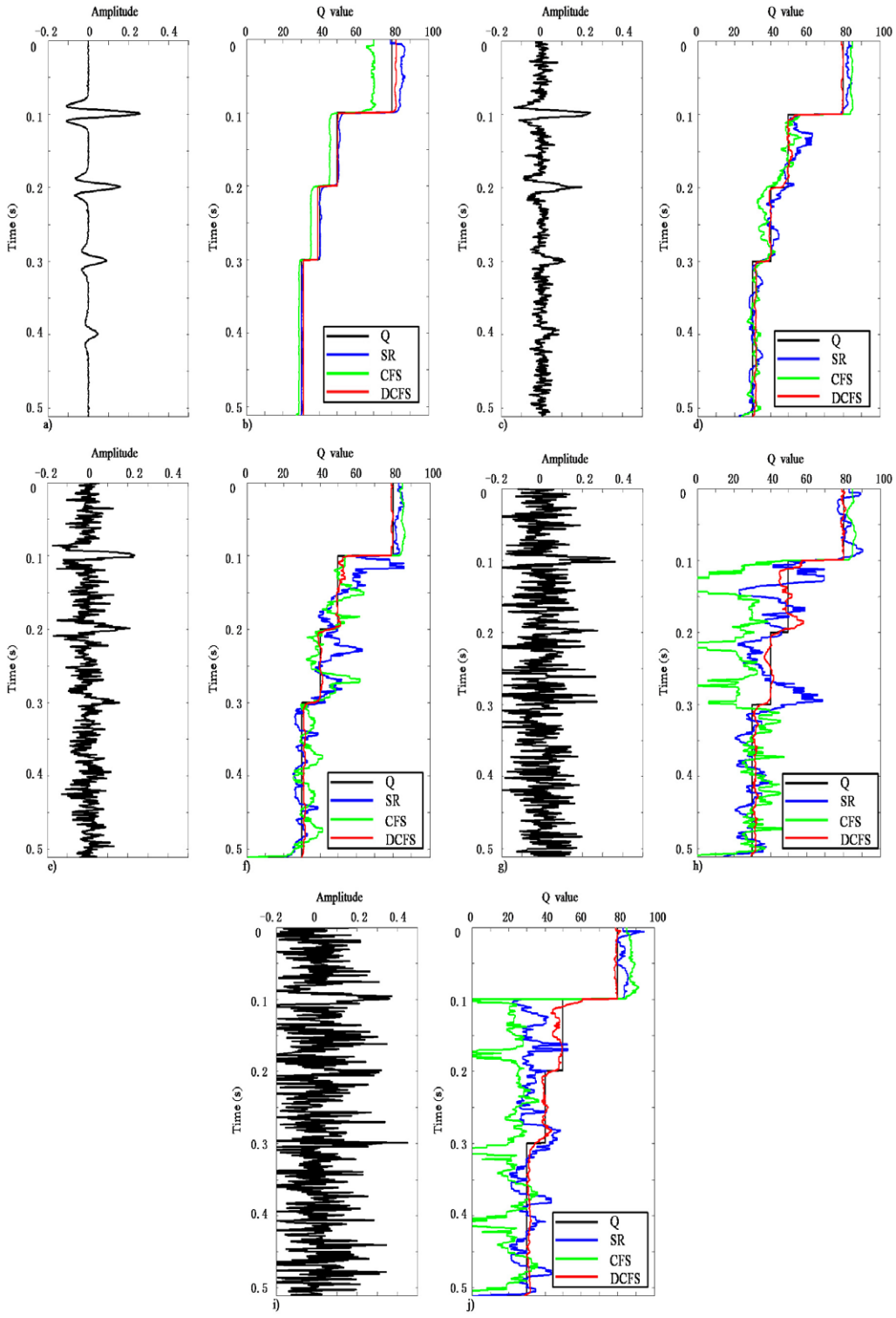

Figure 3. Comparison between SR, CFS, and DCFS methods for synthetic data (same as figure 2(a)) with added random noise. (a), (c), (e), (g), and (i), respectively, show the synthetic data with SNR = 30, 10, 5, 0, and −1 dB. (b), (d), (f), (h), and (j) show the corresponding results of the Q estimation using SR, CFS, and DCFS methods. Note that the results determined by the DCFS method are closer to the true Q values than those of the other two methods with decreasing SNR.

Numerical test and error analysis

Systematic and random errors are the key factors to influence the accuracy and robustness in most methods of Q estimation. As shown in figure 4, we used three methods to estimate the Q value for the fourth layer of the synthetics (figure 2), and the independent experiments were performed 100 times in different SNR (30, 10, 5, 0, and −1 dB) situations. The experiments show that with increasing SNR, the DCFS method performs with the best robustness compared to SR and CFS

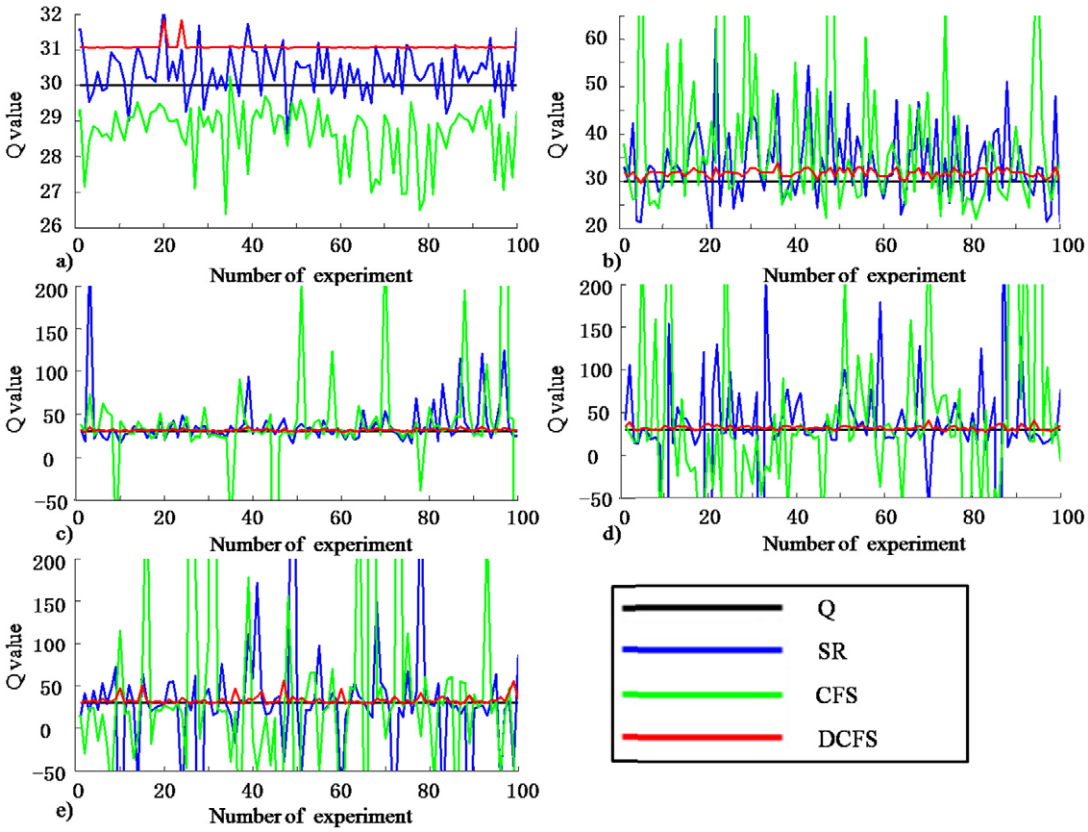

Figure 4. Estimation results of 100 independent experiments for the same layer of the synthetics with SNR = 30 (a), 10 (b), 5 (c), 0 (d), and −1 dB (e) using SR, CFS, and DCFS methods. The actual Q value is 30. Note that the results of the estimation, as denoted by red curves, show that the DCFS method has the best robustness.

methods, as highlighted by the red curve in each figure. However, the negative Q value has appeared in the case of low SNR when using the SR and CFS methods, as shown in figures 4(d) and (e).

For the same attenuated layer with a real Q value 30, we performed independent experiments 100 times in different situation of SNR (30, 10, 5, 0, and −1 dB, respectively). The analysis of the statistical data shown in table 1 also demonstrates that the mean value applied by DCFS is closer to the actual Q value 30, and the standard deviations have no obviously large fluctuation, especially when the noise level is greater than the effective signal (SNR = −1 dB), whereas the abnormally large values of the mean and standard deviation using SR and CFS methods imply that these two methods have less robustness in situations with low SNR compared to our proposed method (DCFS).

Through the error analysis of independents experiments, we found that the relatively accurate estimation results obtained by DCFS are mainly due to the following reasons. First, the central frequency was calculated only one time in the DCFS method, rather than twice in the CFS method, when we used equation (15) to evaluate the Q value; however, SR is easily influenced by noise. This means that the DCFS method decreases the probability of producing the error compared to CFS, and it builds the simple approximate relation between Q, central frequency, and known dominant frequency. Second, DCFS is free from the variance estimation of the reference spectrum in CFS. It seems impractical to assume the Gaussian distribution amplitude spectrum in the CFS method. Also, in CFS, the variances of reference and received spectra are hypothesized to be the same, which intentionally ignores the attenuation effect.

Table 1. Statistical data calculated by 100 experiments using SR, CFS, and DCFS methods. The actual Q value is 30. SD denotes the standard deviation.

	SR		CFS		DCFS	
SNR(dB)	Mean	SD	Mean	SD	Mean	SD
30	30.38	0.56	28.60	0.87	31.20	0.15
10	32.32	7.25	34.53	13.52	31.53	0.85
5	38.54	29.30	39.37	42.41	31.84	3.25
0	159.77	1540	28.36	89.35	32.36	3.28
− 1	52.17	209.28	308.95	3103	32.63	3.65

Application to the field data

To test the validity of our method, we applied the proposed method (DCFS) to a 3D land survey acquired in western China showing the value in detecting a gas reservoir. In figure 5, we analyzed the well data and show the gas reservoir distribution, lithology, and well logs (e.g. GR (natural gamma ray), RT (true formation resistivity), AC (acoustic) and DEN (density)) through three joint wells, which demonstrate that the sandstone is full of the gas reservoir displayed by yellow

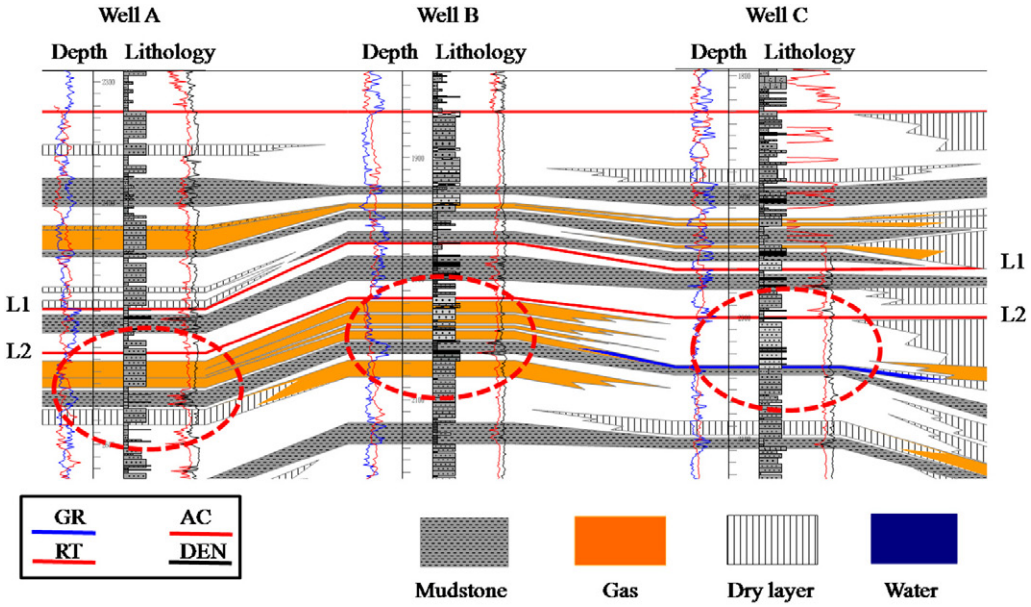

Figure 5. The gas reservoir distribution, lithology, and well logs (e.g. GR, RT, AC, and DEN) through three joint wells. The red ovals denote the compared zones under target layer L2.

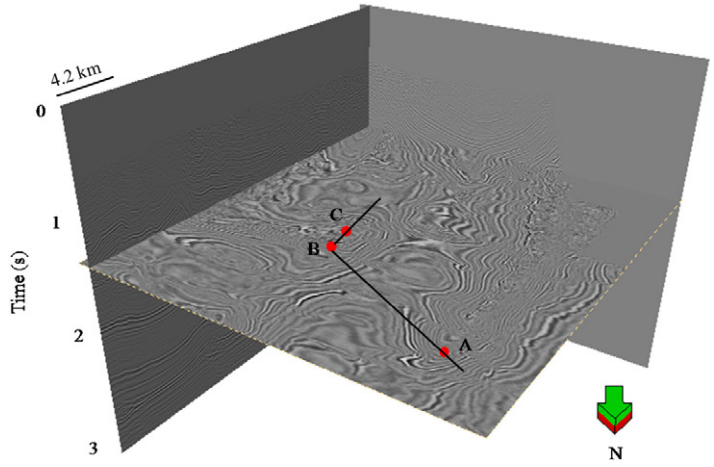

Figure 6. The configuration of the 3D land survey. Red dots show the positions of three wells. Black line denotes a joint well random line.

under layer L2 at wells A and B, whereas there is no oil–gas response at well C. The information from the well logs is used to provide guidance in discriminating the lithological boundaries and indicating the gas reservoir. In addition, we show the visual configuration of 3D land survey and a random line crossing the wells, and denote the positions of three joint wells in figure 6.

For Q estimation in field data, figure 7(a) shows a vertical amplitude slice crossing three wells, as denoted by the black line in figure 6, wherein wells A and B are productive wells and well C is nonproductive. The sampling interval is 1 ms. In the continuous Q profile of figure 7(b) calculated by DCFS using equations (15) and (20), it can be observed that low Q values of the target layer L2 are obviously highlighted by the red curve at the location of productive wells A and B, which implies strong absorption or attenuation in the gas-bearing sandstone, and that this is not a characteristic at the nonproductive well C. The gas distribution denoted by the red ovals from the well logs (figure 5) is consistent with Q value estimation results (figure 7(b)). To further show the advantage of the DCFS method, we used the 20 ms downward time window along the strata L2 to calculate the average Q value shown in figure 7(c). The Q estimation demonstrates that although the results using the three methods (SR, CFS, and DCFS) in this article have similar tendencies in general, the most reasonable Q value estimation is found using DCFS (red dashed curve). The results obtained by the proposed method successfully distinguish productive well B and dry-hole well C, whereas those using SR (blue curve) and CFS (green curve) methods do not show obvious differences between well B and well C. Similarly, we also used the 10 ms downward time window along the strata L1 to calculate the average Q value shown in figure 7(d); no obvious differences in Q values occurred when three methods were applied to measure the attenuation of the mudstone strata with high Q values. Therefore,

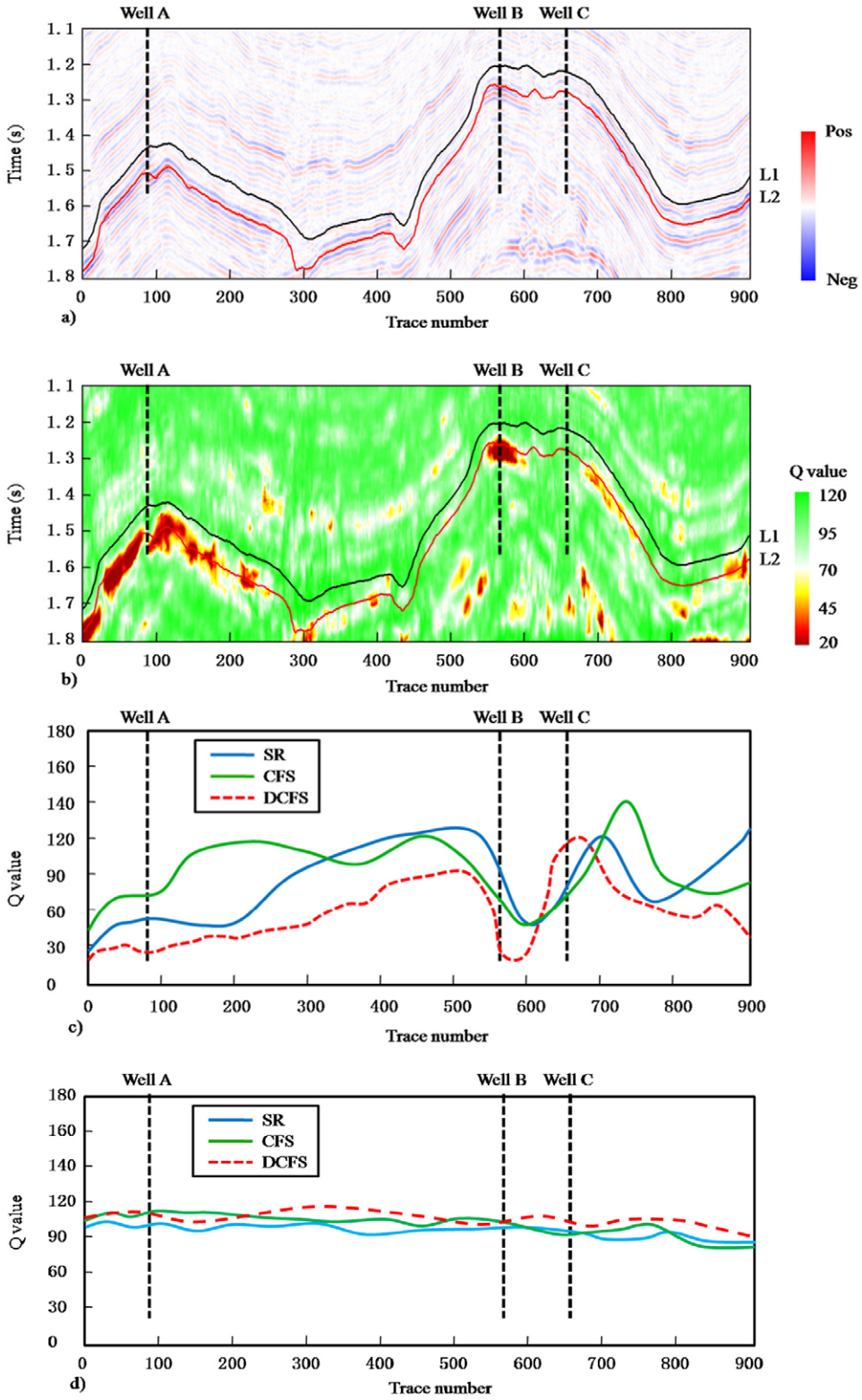

Figure 7. Application to the field data. (a) Vertical profile of seismic amplitude data that cross three joint wells. (b) The continuous Q profile obtained by DCFS method. (c) Estimation of average Q values calculated by SR, CFS, and DCFS methods for target layer L2 within the 20 ms downward time window, and those for (d) layer L1 within the 10 ms downward time window. The most reasonable results using the DCFS method are denoted by a red dashed line in (c).

by analyzing the result calculated by DCFS, the reasonable range of Q values implies that the low Q value area corresponds well to the gas reservoir, whereas the nonproductive well is identified by a high Q value.

Conclusions

This article proposes a novel method for Q estimation based on the assumption of the non-Gaussian amplitude spectrum of

Ricker wavelet, wherein a simple and effective Q approximate equation is built between dominant frequency and central frequency. It not only overcomes the shortage of the SR method, which is highly dependent on the SNR of seismic data, but also improves the robustness and accuracy of evaluating the Q value compared to the CFS method. The statistical analysis and application to both the synthetic data and field data calibrate the effectiveness of the proposed DCFS method and also confirm that the results calculated by DCFS are reliable and provide useful guides in hydrocarbon detection and reservoir characterization.

Acknowledgments

This work is financially supported by the National Natural Science Foundation of China (grant no. 41204091), the Science and Technology Support Program (grant no. 2011GZ0244), and the Science and Technology Department of Sichuan Province of China. The second author (corresponding author) appreciates the Chinese Scholarship Council for financial support. The authors also thank Zhongyuan Oilfield of SINOPEC for providing the field data.

References

Barnes A E 1991 Instantaneous frequency and amplitude at the envelope peak of a constant-phase wavelet *Geophysics* **56** 1058–60

Brzostowski M and McMechan G 1992 3D tomographic imaging of near-surface seismic velocity and attenuation *Geophysics* **57** 396–403

Clark R A, Carter A J, Nevill P C and Benson P M 2001 Attenuation measurements from surface seismic data—Azimuthal variation and time lapse case studies *63rd Conf. and Technical Exhibition, EAGE, Expanded Abstracts* p L-28

Engelhard L 1996 Determination of seismic-wave attenuation by complex trace analysis *Geophys. J. Int.* **125** 608–22

Hauge P S 1981 Measurements of attenuation from vertical seismic profiles *Geophysics* **46** 1548–58

Hedlin K, Mewhort L and Margrave G 2001 Delineation of steam flood using seismic attenuation *SEG Expanded Abstr.* **20** 1572–5

Hu C H, Tu N and Lu W K 2013 Seismic attenuation estimation using an improved frequency shift method *IEEE Geosci. Remote Sens. Lett.* **10** 1026–30

Kaderali A, Jones M and Howlett J 2007 White Rose seismic with well data constraints: a case history *Leading Edge* **26** 742–54

Kjartansson E 1979 Constant Q-wave propagation and attenuation *J. Geophys. Res.* **84** 4737–48

Korneev V A, Goloshubin G M, Daley T M and Silin D B 2004 Seismic low-frequency effects in monitoring fluid-saturated reservoirs *Geophysics* **69** 522–32

Li H B, Zhao W Z, Cao H, Yao F C and Shao L Y 2006 Measures of scale based on the wavelet scalogram with applications to seismic attenuation *Geophysics* **71** 111–8

Luh P C 1993 Wavelet attenuation and AVO *Offset-Dependent Reflectivity: Theory and Practice of AVO Analysis (Investigations in Geophysics* vol 8*)* ed J P Castagna and M M Backus (Tulsa, OK: Soc. Expl. Geophys.) pp 190–8

Matheney M P and Nowack R L 1995 Seismic attenuation values obtained from instantaneous frequency matching and spectral ratios *Geophys. J. Int.* **123** 1–15

Maultzsch S, Chapman M, Liu E and Li X Y 2007 Modelling and analysis of attenuation anisotropy in multi-azimuth VSP data from the Clair field *Geophys. Prospect.* **55** 627–42

Parra J O and Hackert C L 2002 Wave attenuation attributes as flow unit indicators *Leading Edge* **21** 564–72

Quan Y and Harris J M 1997 Seismic attenuation tomography using the frequency shift method *Geophysics* **62** 895–905

Raikes S A and White R E 1984 Measurements of earth attenuation from downhole and surface seismic recordings *Geophys. Prospect.* **32** 892–919

Rein C, Van Dan Baan M and Clark R 2009 The robustness of seismic attenuation measurement using fixed and variable-window time-frequency transform *Geophysics* **74** WA123–35

Ricker N 1953 The form and laws of propagation of seismic wavelets *Geophysics* **18** 10–40

Sams M S and Goldberg D 1990 The validity of Q estimates from borehole data using spectral ratios *Geophysics* **55** 97–101

Singleton S, Taner M T and Treitel S 2006 Q estimation using Gabor–Morlet joint time-frequency analysis techniques *SEG Extended Abstr.* **25** 1610–4

Toksöz M N, Johnston D H and Timur A 1979 Attenuation of seismic waves in dry and saturated rocks: I. Laboratory measurements *Geophysics* **44** 681–90

Tonn R 1991 The determination of the seismic quality factor Q from VSP data: a comparison of different computational methods *Geophys. Prospect.* **39** 1–27

Wang Y 2002 A stable and efficient approach of inverse Q filtering *Geophysics* **67** 657–63

Wang Y 2004 Q analysis on reflection seismic data *Geophys. Res. Lett.* **31** L17606

Wang Y 2006 Inverse Q-filter for seismic resolution enhancement *Geophysics* **71** V51–60

Wang Y 2008 *Seismic Inverse Q Filtering* (Malden: Blackwell)

Wang Y 2014 Stable Q analysis on vertical seismic profiling data *Geophysics* **79** D217–25

Wang Y 2015 Frequencies of the Ricker wavelet *Geophysics* **80** A31–7

White R E 1992 The accuracy of estimating Q from seismic data *Geophysics* **57** 1508–11

Winkler K W and Nur A 1982 Seismic attenuation—effects of pore fluids and frictional sliding *Geophysics* **47** 1–15

Wright C and Hoy D 1981 A note on pulse broadening and anelastic attenuation in near-surface rocks *Phys. Earth Planet. Inter.* **25** P1–8

Zhang C J and Ulrych T J 2002 Estimation of quality factors from CMP records *Geophysics* **67** 1542–7

Zhu Y and Tsvankin I 2007 Plane-wave attenuation anisotropy in orthorhombic media *Geophysics* **72** D9–19